Task: MAG-S.01.06-T013

EU-CN Analysis of AC losses and thermal – hydraulic simulations (2025)

Monika LEWANDOWSKA, Aleksandra DEMBKOWSKA, Rafał ORTWEIN

IPPLM / The Henryk Niewodniczański Institute of Nuclear Physics
Polish Academy of Sciences, Kraków, Poland

WMAG Final Meeting 2025, Villigen PSI, 15 January 2026

Task specification

Description:

Thermal-hydraulic simulations of normal operation of CORC conductor(s) (CN design) using the THEA code will be performed. Simulations with ANSYS APDL (3D solid + 1D fluid) of the behaviour of short lengths of the considered CORC conductor(s) are also possible.

Outline

- Goal of the study
- Input data
- Magnetic flux distribution within the CS coil
- THEA model
- AC losses evaluation
- Results and discussion
- Summary and conclusion

Goal of the study

- Estimation of the global minimum temperature margin during normal operation of the BEST HTS CORC CS conductors and verification if it fulfills the acceptance criterion:

  $\min \Delta T_{marg} > 1.5$ K

  where $\Delta T_{marg}(x,t) = T_{cs}(x,t) - T_{sc}(x,t)$

  x - curvilinear coordinate along a conductor

  T_{cs} - current sharing temperature

  T_{sc} - superconductor temperature

- Estimation of the maximum hot spot temperature margin during quench of the BEST HTS CORC CS conductors and verification if it fulfills the acceptance criterion:

  $\max T_{jacket} > 150$ K

Input data – BEST CS coils and HTS conductor geometry

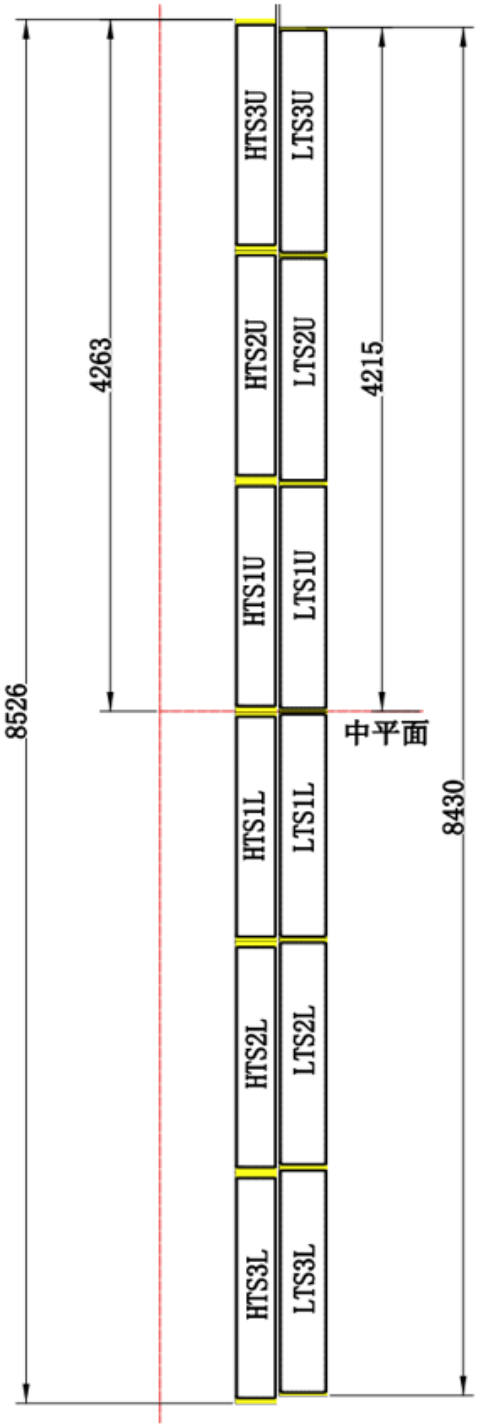

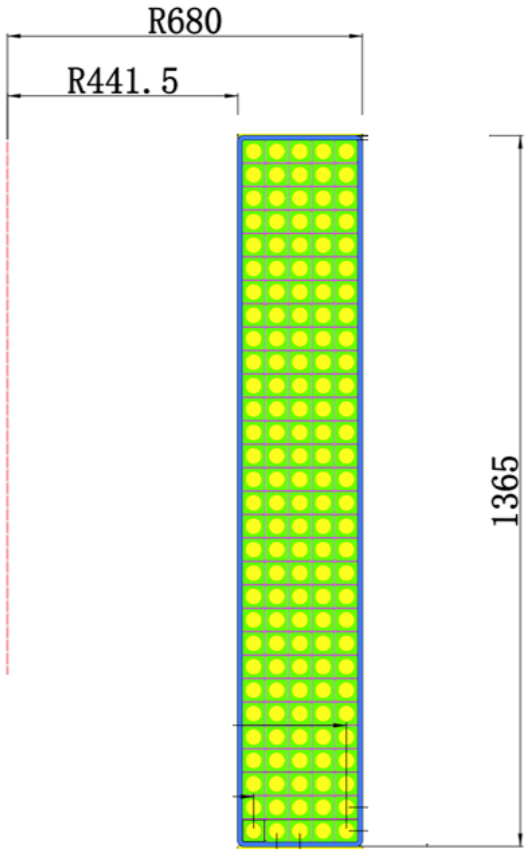

HTS module

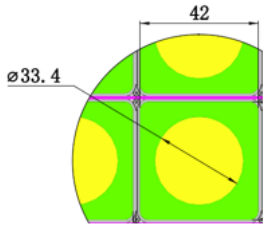

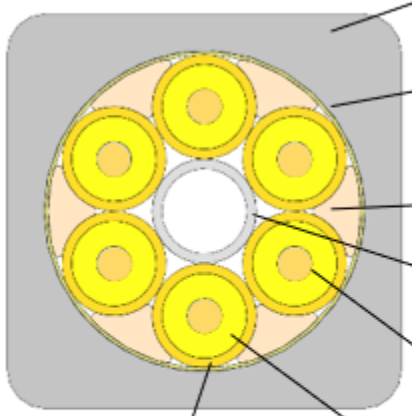

Jacket: OD: 42.5×42.5 mm
ID：φ33.8mm

Overbanding tape：OD：33.8
(SSS) ID： 32.7

Cu block：21.98 mm²

Central tube：OD：10.9 mm
ID：8.88 mm

Cu core: OD:4.6 mm

Copper tube:
OD:10.9mm ID:8.88 mm

cable area: ID:4.6mm OD:8.88 mm
Contains:
SC cross sectional area: 28.5 mm²
Cu tape cross sectional area: 7.1 mm²

- Max. operating current: 46.5 kA
- Number of HTS tapes: 288
- HTS tapes width: 4 mm
- He cross section (central channel): 28.74 mm²
- He cross section (6 triangle channels): 28.74 mm²

Input data – cooling conditions

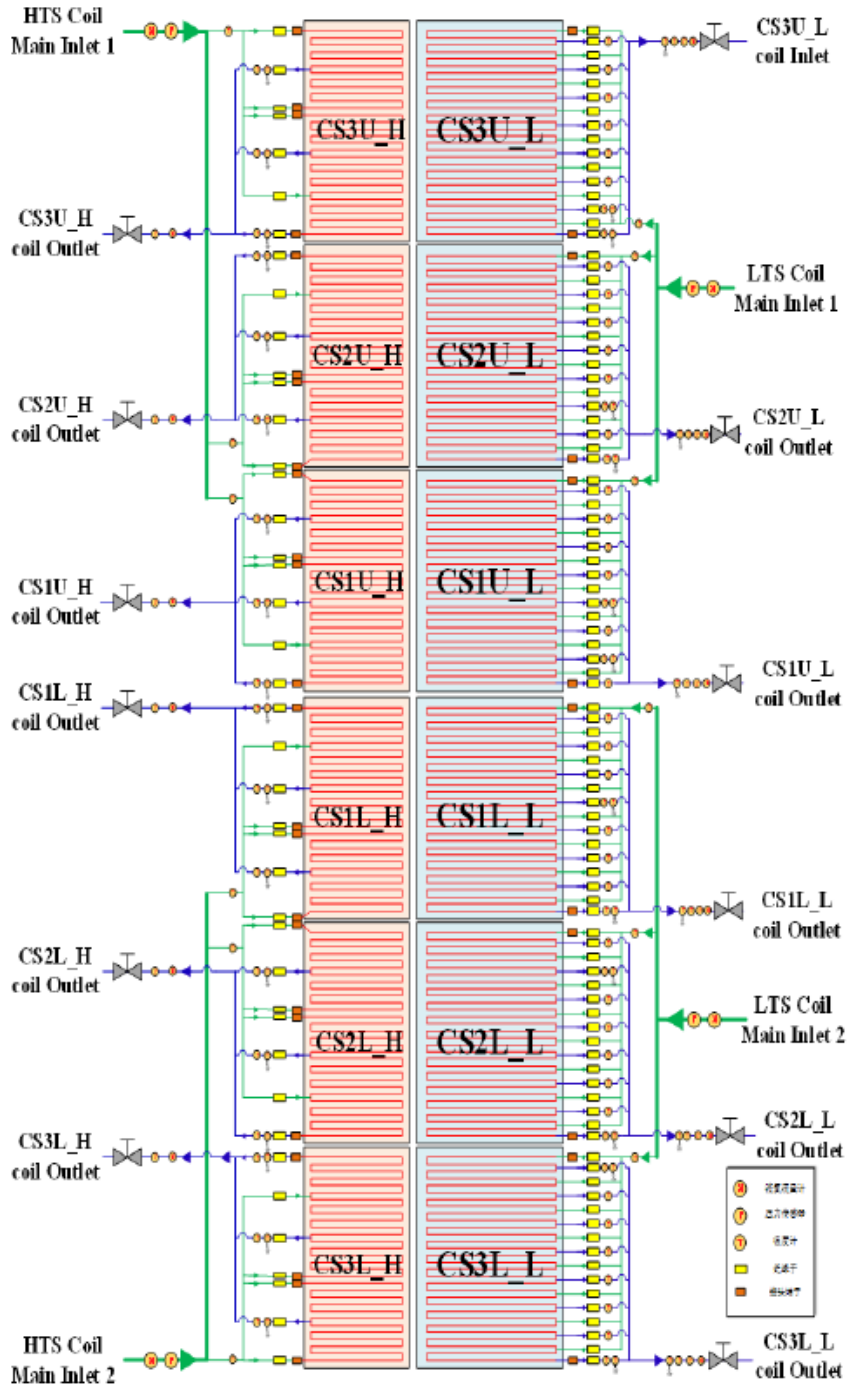

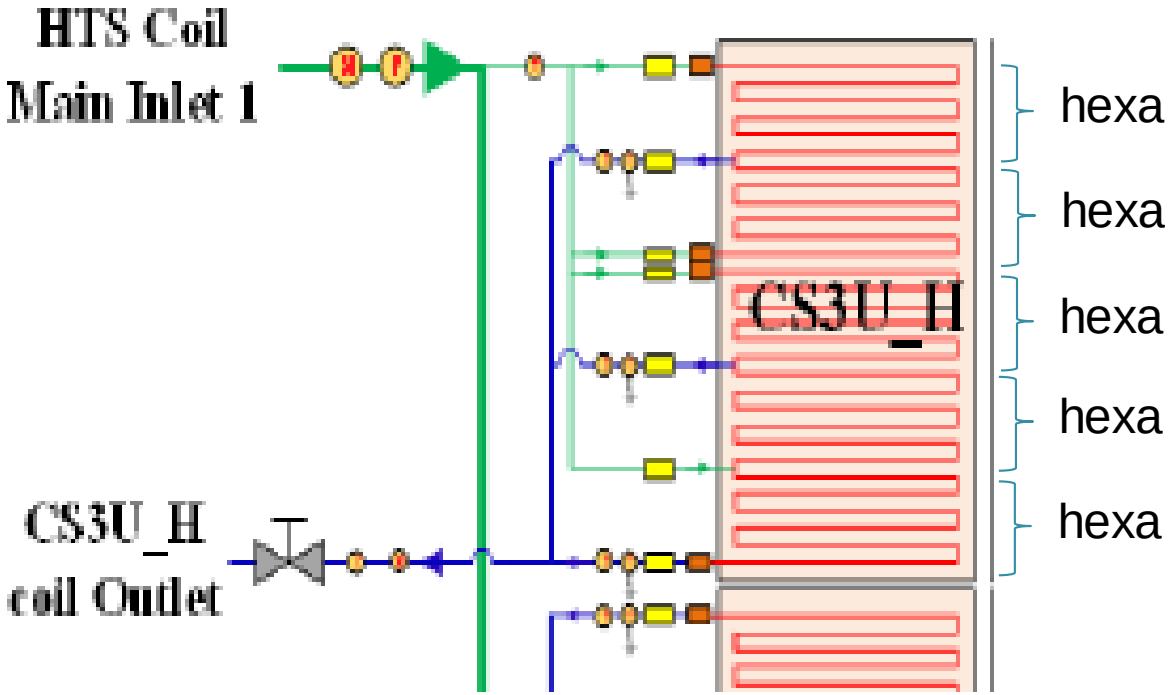

He inlet pressure: 5 bar

He inlet emperature: 4.2 K

Nominal mass flow rate: 14 g/s (at no heat load)

5 Hexa-pancakes in each HTS module

5 Turns in each pancake

Hydraulic length ~ 106 m

Input data – current scenario

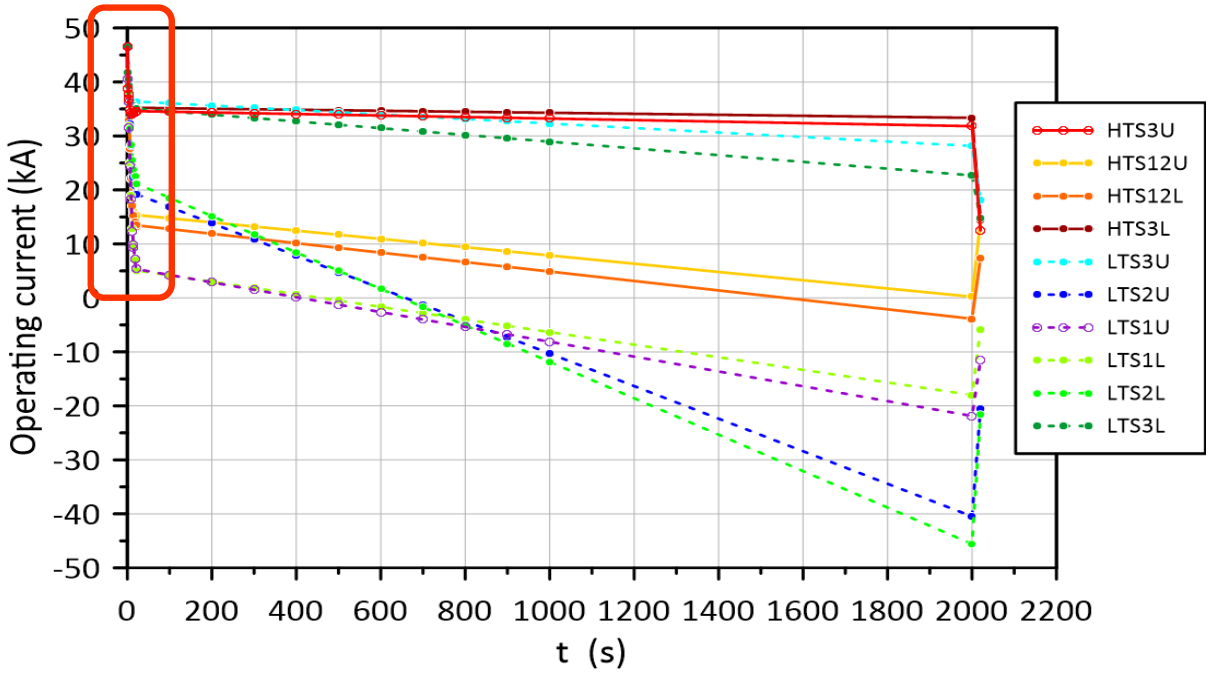

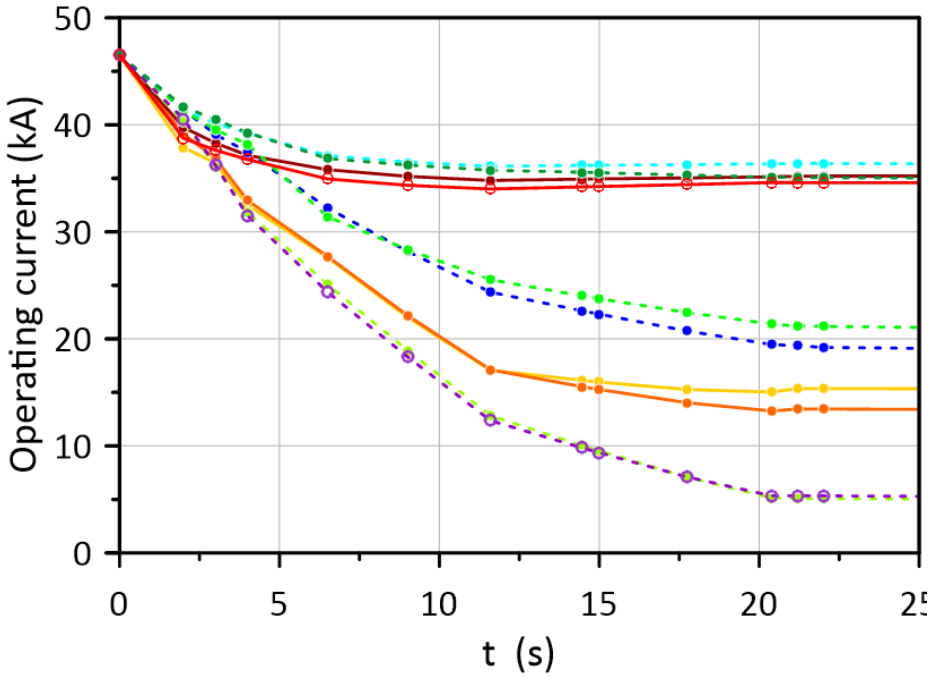

We developed an axisymmetric model of the CS in the ANSYS APDL environment to calculate the magnetic field distribution within the CS at 10 (out of 25) time points selected from the current scenario (namely: t = 0, 2, 3, 4, 6.5, 11.4, 20.4, 22, 2000, and 2020 s), between which the operating current in CS conductors varied almost linearly.

Magnetic field evolution in the CS modules

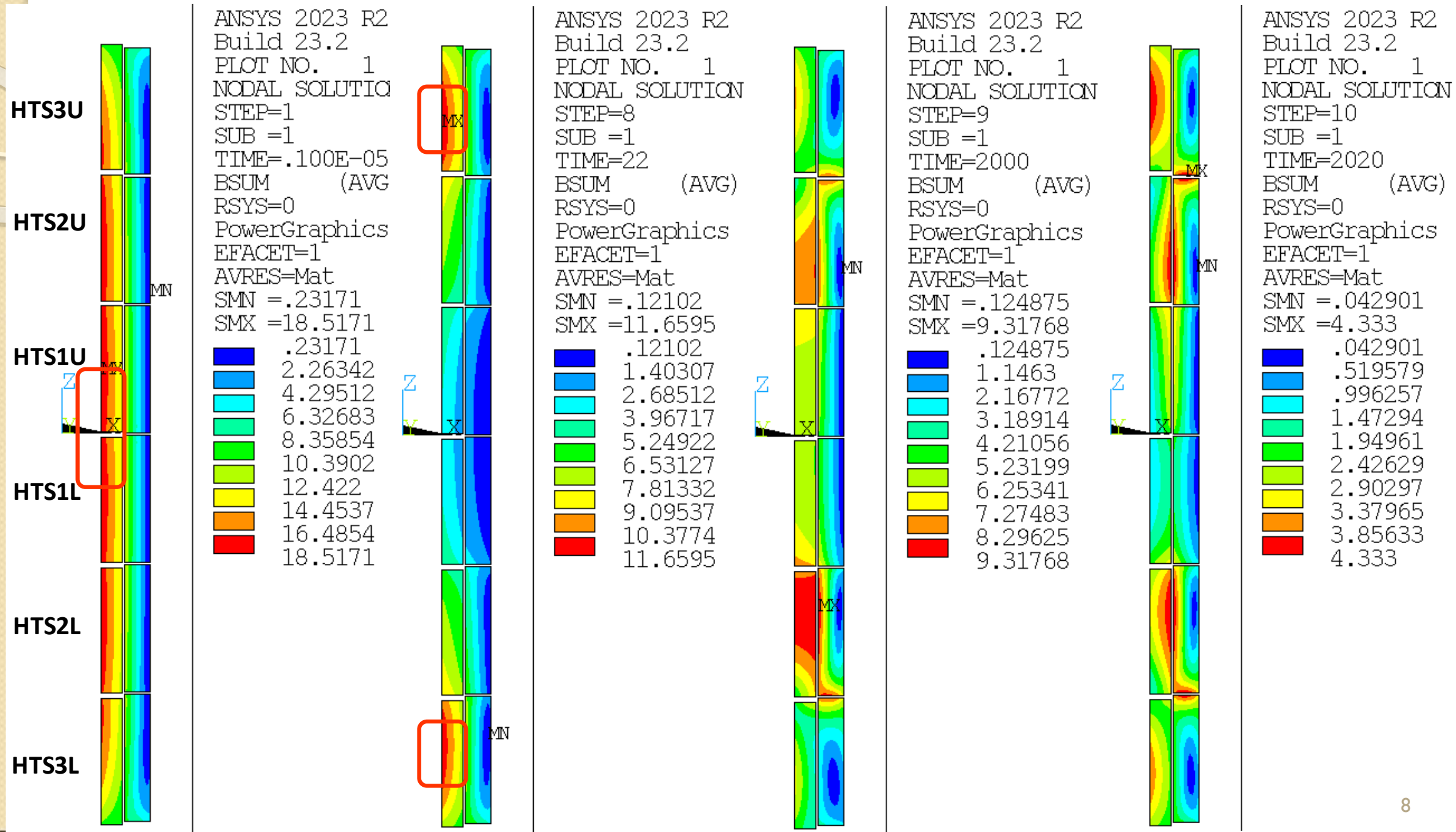

Transformation of the 2D MF distribution into 1D MF profiles along the cables

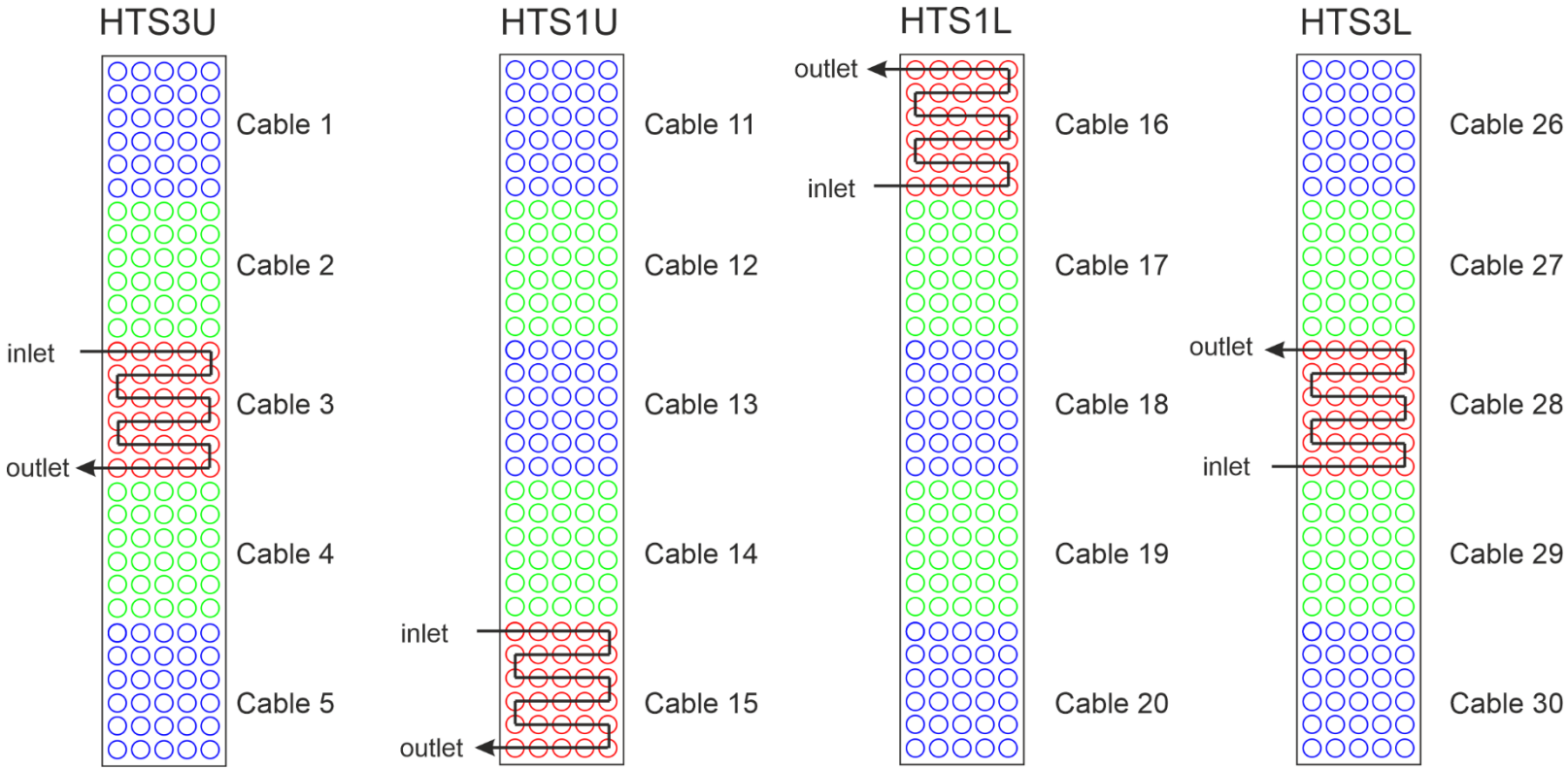

Based on the results of the electromagnetic analysis, 4 cables (cables 3, 15, 16, and 28 counting from the top of the CS), which under operating conditions were subjected to particularly high MF, or its fastest changes, were selected for further analysis (cables 15 and 16 are expected to be the most critical).

For the selected cables the magnetic field profiles along the cables at the 10 successive characteristic time points of the current scenario were determined.

MF profiles along the selected cables

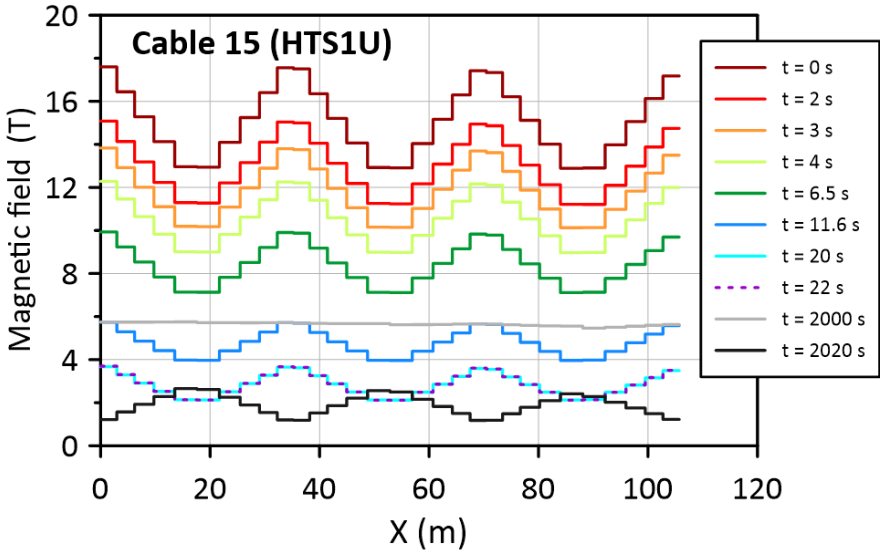

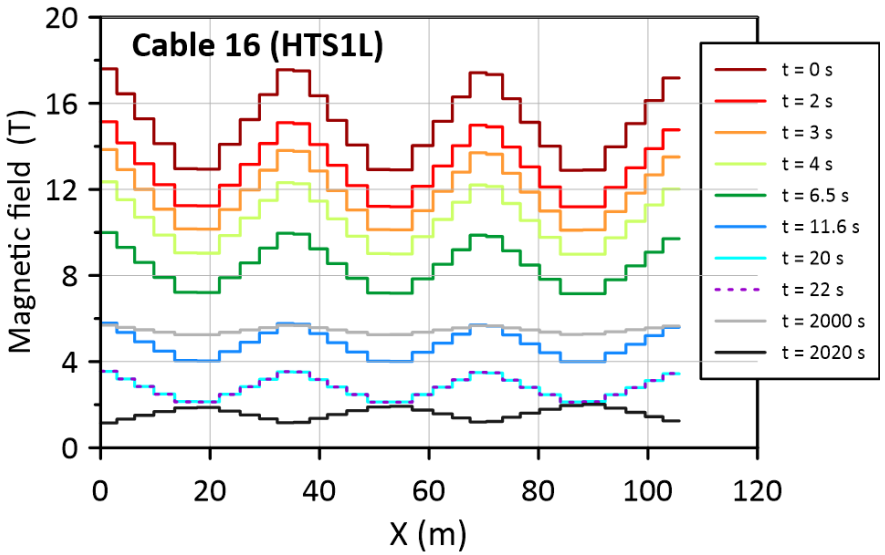

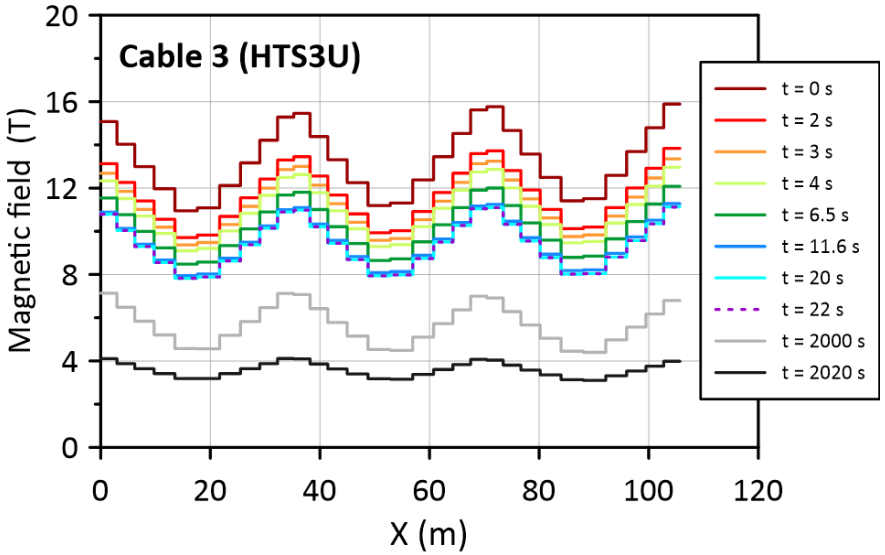

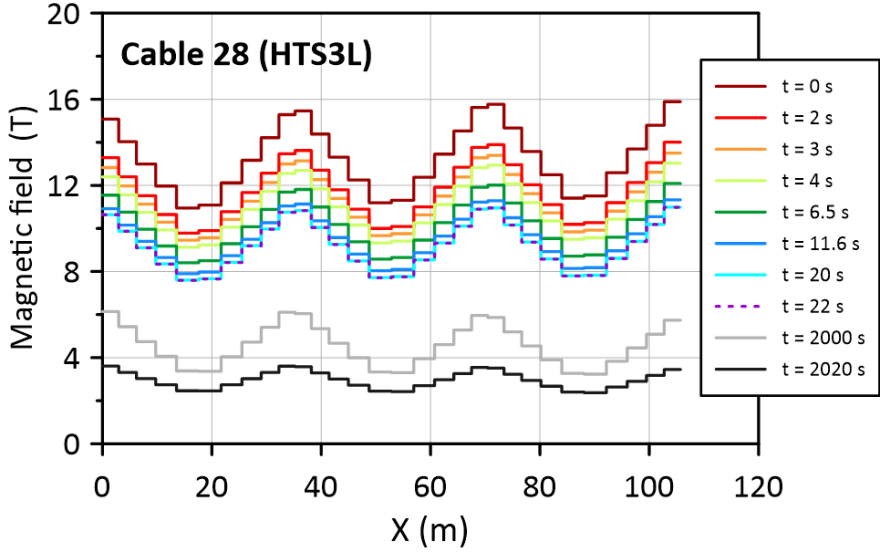

For times between the given points of the current scenario the MF was obtained by linear interpolation.
Variations of MF in the first seconds of the current scenario are much faster than those observed in the DEMO CS conductors.

THEA model – 1D conductor components

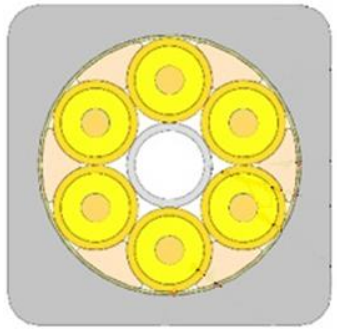

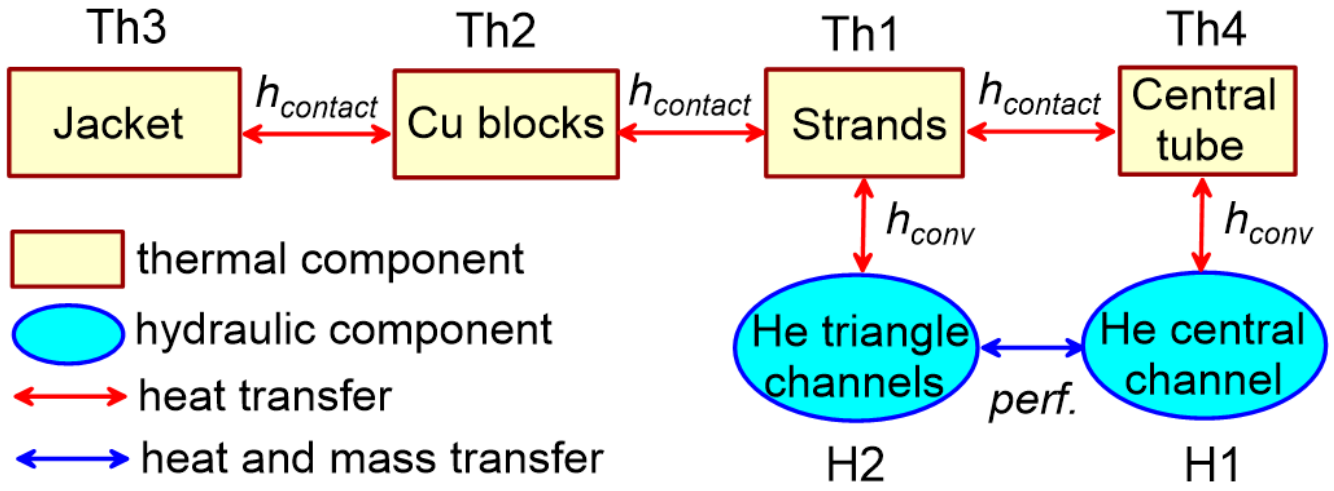

Conductor components in the THEA model and thermal links between them

- Assumed cooling conditions: T_{in} = 4.2 K, p_{in} = 5 bar, we selected p_{out} = 4.774 bar to ensure the correct nominal mass flow rate of 14 g/s
- Thermal links between the conductor components were assumed as in TH simulations of the EU-DEMO conductors [1]:
  - Standard friction factor and heat transfer correlations for flow in the central tube and triangle channels,
  - Contact heat transfer coefficient between the solid cable components $h_{contact}$ = 500 W/(m^{2}K),
  - Perforation of the central tube ~1.5%.

[1] L. Savoldi and R. Zanino, Common approach for thermal-hydraulic calculations, Memo for WPMAG-2.1-D01 (2016) EFDA_2LMECE

THEA model – I_c (B,t) scaling laws for SST tapes

- In the preliminary simulations, performed in the scope of our 2024 task, we used the scaling law given by:

$$I_{c1}(B,T) = n_t \cdot 2066.52 \cdot B^{-0.55666} \cdot \exp\left(\frac{-T}{39.2586 - 0.80338 \cdot B}\right)$$

which turned out to be very inaccurate at low MF and low operating currents ($T_{cs} > T_c$).

- In the present study we use the following scaling law for SST tapes [2]:

$$I_{c2}(B,T) = \frac{F_{p0}}{B}\left[\frac{B}{B^*_{sc}(T)}\right]^p \left[1 - \frac{B}{B^*_{sc}(T)}\right]^q$$

$$F_{p0}(T) = A_0\left[1 - \left(\frac{T}{T_c}\right)^\beta\right] B^*_{sc}(T)^\nu$$

$$B^*_{sc}(T) = B_{sc0}\left[1 - \left(\frac{T}{T_c}\right)^\alpha\right]^\mu$$

B ⊥ tapes surface

A_0=21.24 AT$^{1-\nu}$/cm, B_{sc0} = 187.7 T, T_c=92 K, β=6.87, α = 0.514, μ = 1.496, ν = 1.514, p = 0.521, q = 1.9 which can be considered as a very conservative [3,4].

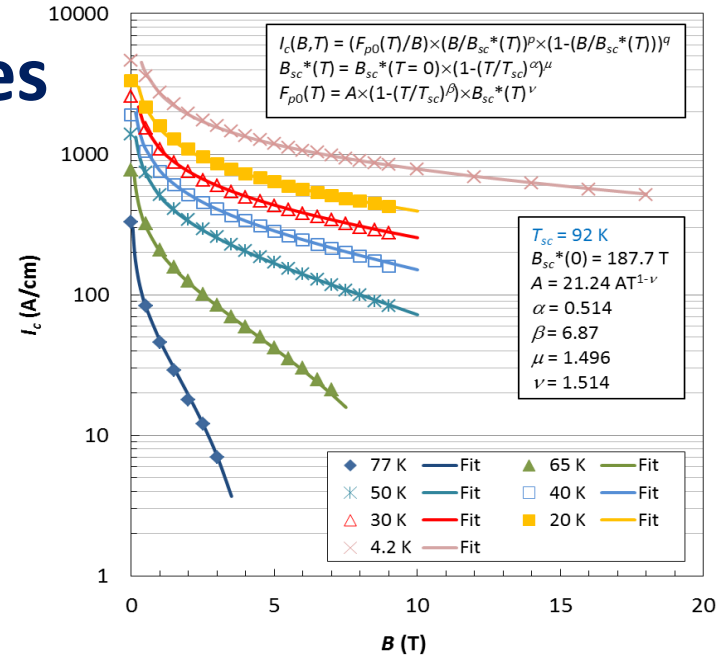

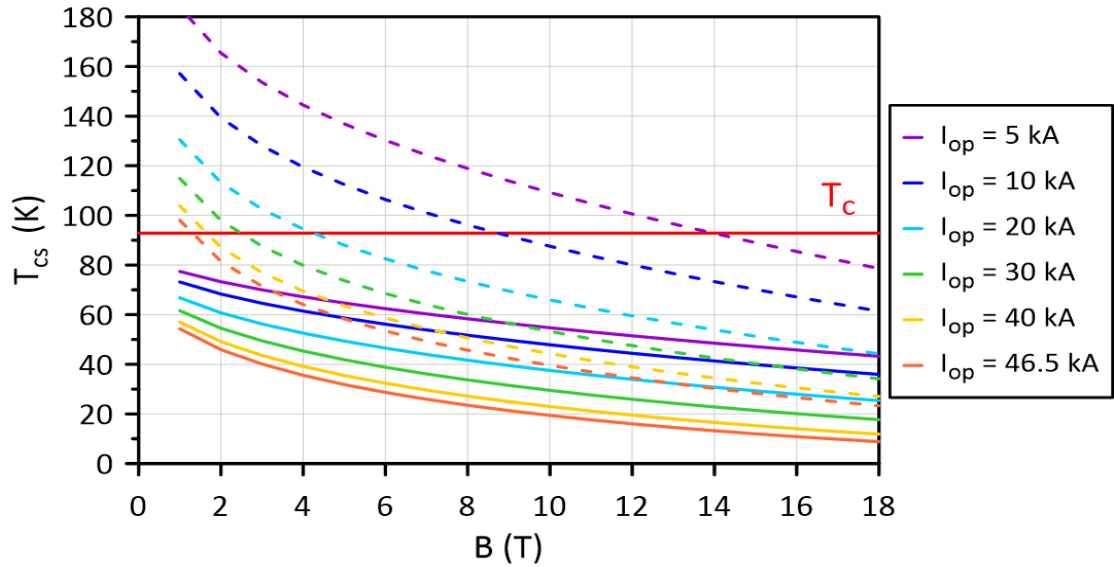

T_{cs} values predicted by both scaling laws; I_{c1} - dashed lines, I_{c2} - solid lines

[2] R. Wesche: Ic(B,T) Scaling of Coated Conductors, EPFL-SCP internal report, May 2017

[3] G. Succi, et al.: Magnetic Field and Temperature Scaling of the Critical Current of REBCO tapes, IEEE Trans. Appl. Supercon. 34 (2024) 8001007

[4] C. Senatore, et al.: REBCO tapes for applications in ultra-high fields: critical current surface and scaling relations. Supercond. Sci. Technol. 37 (2024)

THEA model - heat loads: hysteresis losses

The magnetization loss (in kJ/m³/cycle, normalized to the HTS tapes volume) was calculated based on the experimental fit obtained for the CORC conductor designed by ASIPP [5]:

$$Q_{hys}(B) = \begin{cases} c_1 B^3 & \text{for } 0 < B < 0.903 \text{ T} \\ aB^6 + bB^5 + cB^4 + dB^3 + eB^2 + fB & \text{for } 0.903 \text{ T} < B < 13.369 \text{ T} \\ a_1 B^{b_1} & \text{for } 13.369 \text{ T} < B < 18 \text{ T} \end{cases}$$

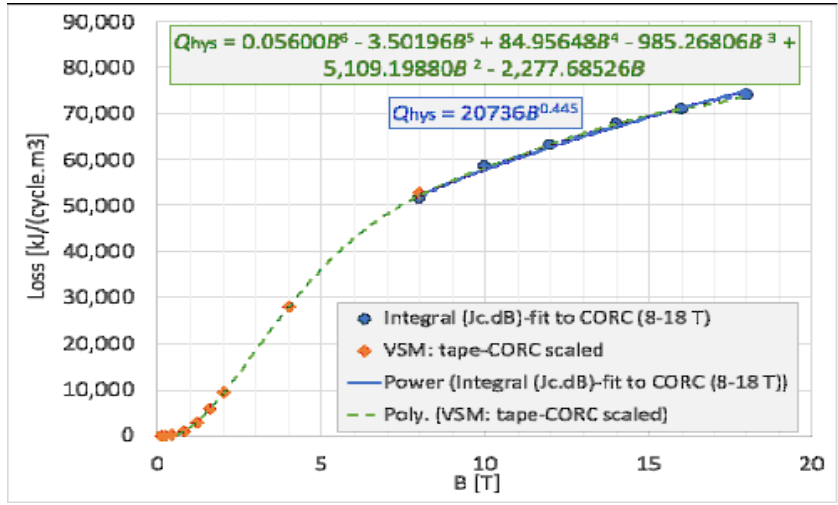

where: a = 0.05600, b = -3.50196, c = 84.95648, d = -985.26806, e = 5 109.19880, f = - 2 277.68526, a_1 = 20736, b_1 = 0.445, c_1 = 1953.4.

The respective expression for the thermal power of hysteresis losses (in kW/m) is:

$$P_{hys}(B) = C_{phase} A_{tapes} \frac{dQ_{hys}}{dt} \qquad C_{phase} = 0.25$$

$$P_{hys}(B) = C_{phase} A_{tapes} \left|\frac{dB}{dt}\right| \begin{cases} 3c_1 B^2 & \text{for } 0 < B < 0.903 \text{ T} \\ 6aB^5 + 5bB^4 + 4cB^3 + 3dB^2 + 2eB + f & \text{for } 0.903 < B < 13.369 \text{ T} \\ a_1 b_1 B^{(b_1 - 1)} & \text{for } 13.369 \text{ T} < B < 18 \text{ T} \end{cases}$$

[5] A. Nijhuis, EU-CN CORC-CICC coupling loss in transverse and parallel AC field, Task MAG-T.01.01-T026-D001 (2023), EFDA_D_2RD8QR

THEA model - Heat loads: coupling and eddy current losses

The coupling loss per unit length of conductor in a field ramped at a uniform rate was calculated as [6]:

$$P_{coupling}(x) = \frac{n\tau S}{\mu_0}\left(\frac{dB(x)}{dt}\right)^2 = \frac{n\tau S}{\mu_0}\left[\left(\frac{dB_r(x)}{dt}\right)^2 + \left(\frac{dB_z(x)}{dt}\right)^2\right]$$

where n - demagnetization factor,

τ - time constant

S – copper cross section in a given thermal component.

The values of $\dot{B}_r(x)$ and $\dot{B}_z(x)$ during the subsequent phases of the current scenario were estimated using the respective $B_r(x)$ and $B_z(x)$ values at the beginning and end of the given phase.

The $n\tau$ values for the considered conductor geometry, taking into account both the coupling and eddy current losses in the copper components, were obtained by Gianluca De Marzi with a dedicated electrostatic FEM model (assuming copper RRR = 50 and the electrical contact resistance between different cable components equal to: $R_c = 3 \cdot 10^{-7}\ \Omega \cdot m$)

$$\boldsymbol{n\tau(B) = -0.0259247 \cdot B^3 + 1.40531 \cdot B^2 - 30.1608 \cdot B + 338.722}$$

(B in T, $n\tau$ in ms)

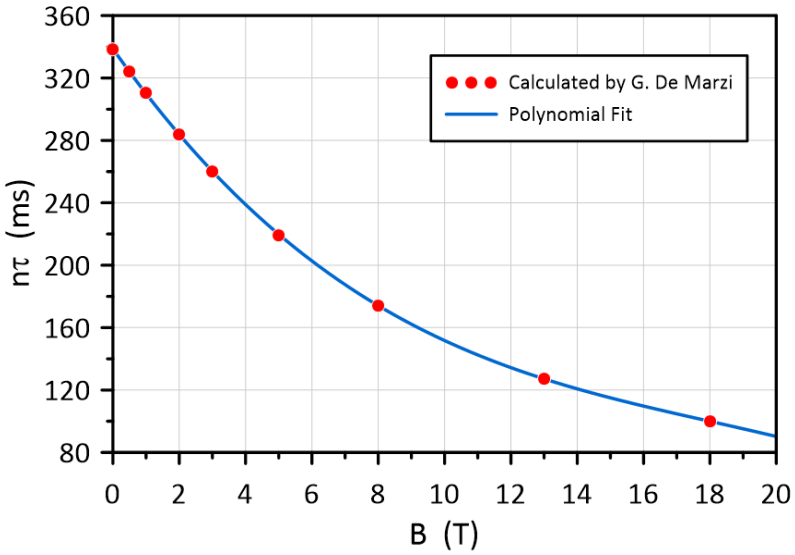

[6] M. N. Wilson, Superconducting Magnets, Clarendon Press 1983.

THEA model - Heat loads: examples

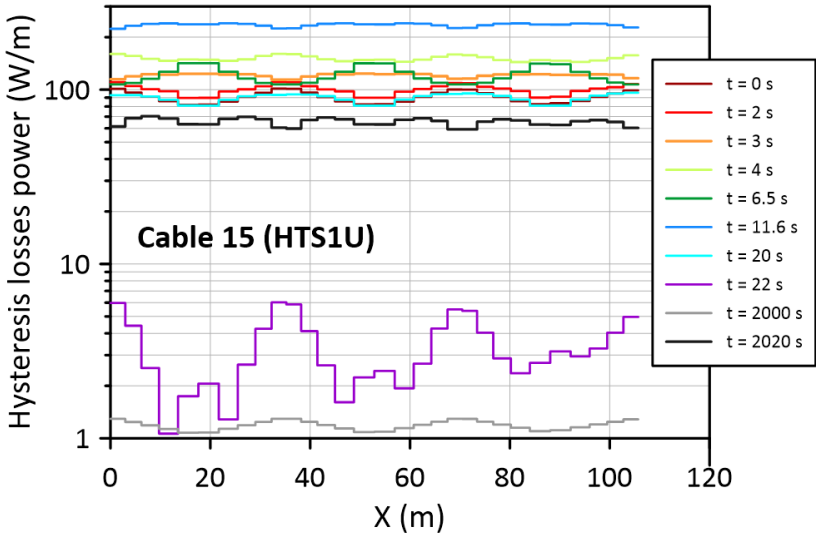

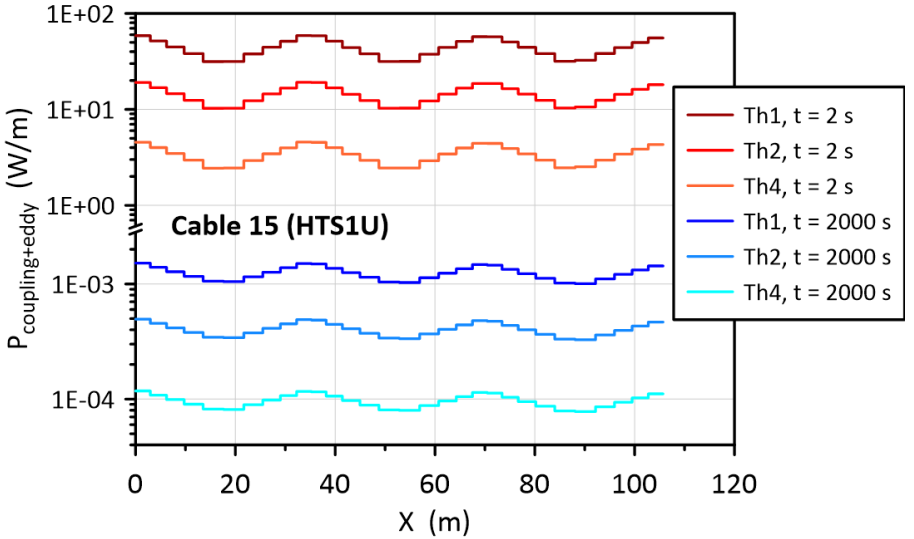

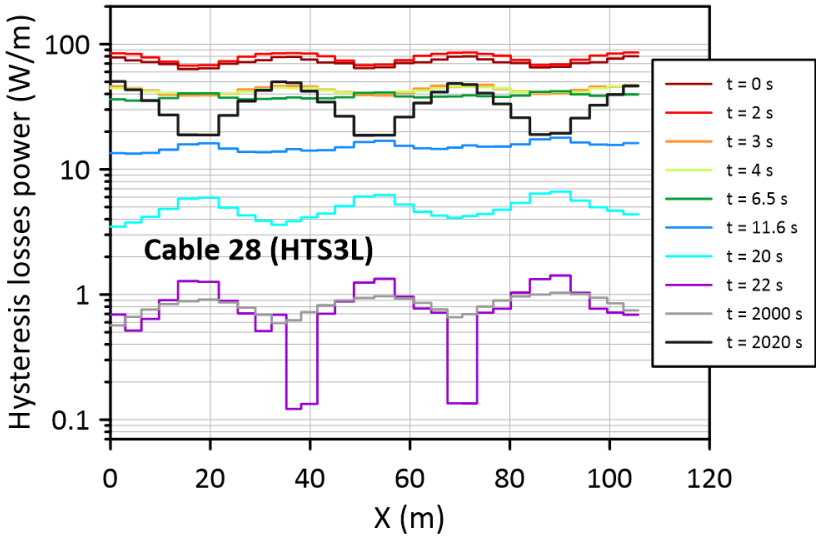

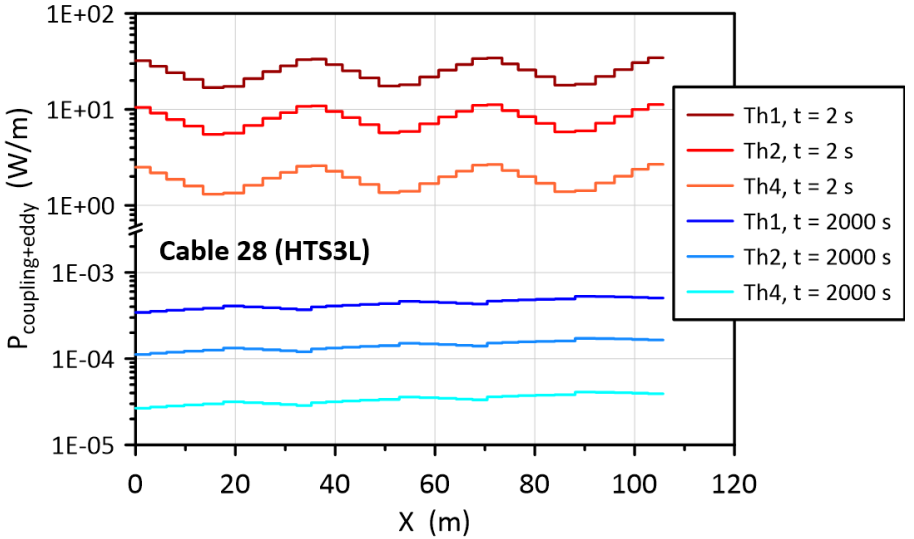

Hysteresis losses in the considered conductors are large, particularly in the first and last few seconds of the current secenario. The coupling and eddy current losses are smaller, but at the beginning of the current scenario they are also quite significant.

THEA model – simulation procedure and model validation

- Preliminary simulations of conductors behaviour at the start of the current scenario:
  - Initial conditions: $T(x) = T_{in}$, $p(x) = p_{in}$, $\dot{m}_{cc}(x) = 12$ g/s, $\dot{m}_{tc}(x) = 3$ g/s
  - Maximum operating current $I_{op} = 46.5$ kA = const and B(x) = B (x,t=0) = const, no heat load
  - Simulations lasted until the stationary state was observed
  - The resulting steady state temperature, pressure and mass flow rate profiles served as initial conditions for the subsequent simulations of the whole curent scenario and quench simulations.
  - The results of the steady state hydraulic analysis as well as the stationary T, p, T_{cs} and ΔT_{marg} profiles obtained with THEA agreed very well with the respective values obtained with the simplified models [7,8]

Parameter	Unit	Value
He mass flow rate in the central channel	g/s	12.47
He velocity in the central channel	m/s	1.44
Re in the central channel	-	$4.48 \cdot 10^5$
He residence time in the central channel	s	73.6
He mass flow rate in the 6 triangle channels	g/s	1.53
He velocity in the triangle channels	m/s	0.38
Re in the triangle channels	-	$1.72 \cdot 10^5$
He residence time in the triangle channels	s	277.9
He outlet temperature	K	4.229

[7] M. Lewandowska, K. Sedlak, Thermal-hydraulic analysis of LTS cables for the DEMO TF coil, IEEE Trans. Appl. Supercon. 24 (2014) Art. No 4200305.

[8] M. Lewandowska, A. Dembkowska, R. Heller, M. Wolf, Thermal-hydraulic analysis of an HTS DEMO TF coil, Cryogenics 96 (2018) 125-132.

THEA model – simulation procedure and model validation

- The THEA conductor model was further validated by comparison T, p, T_{cs} and ΔT_{marg} profiles at the end of burn (t = 2000 s) with the respective predictions of the steady-state model [7,8].
- Given the long duration of the burn phase and relatively low heat loads in this phase, at t = 2000 s the stationary state was reached, thus the results obtained with THEA code were in very good agreement with the predictions of the simplified model .

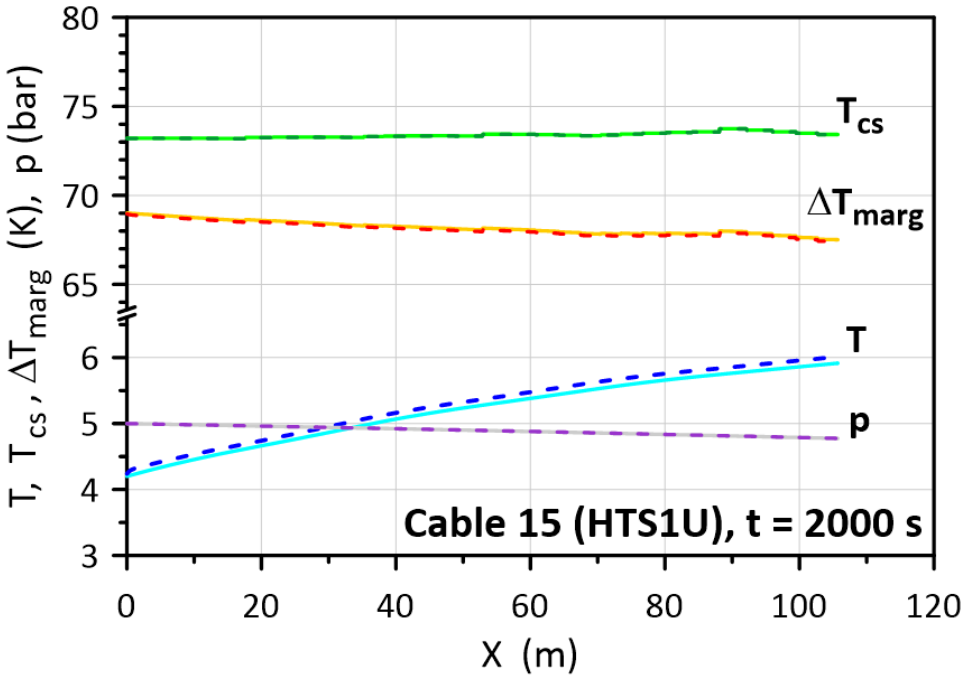

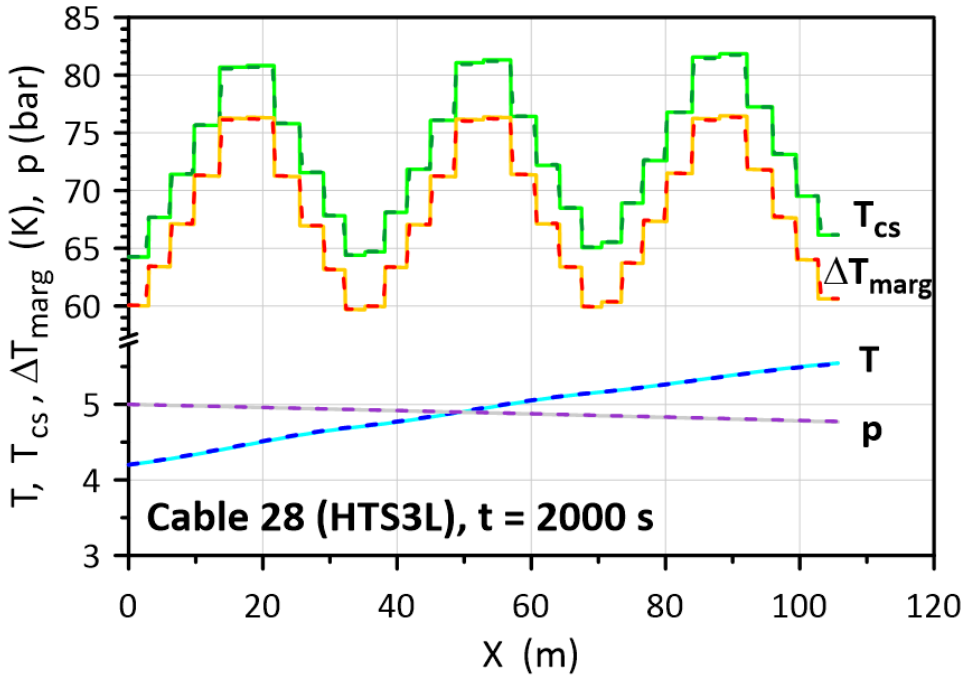

Comparison of the THEA results (dashed lines) with the respective results obtained with the simplified steady state model [7,8] (solid lines)

Results – typical time evolution of T, T_{cs} and ΔT_{marg} profile at the beginning of the current cycle

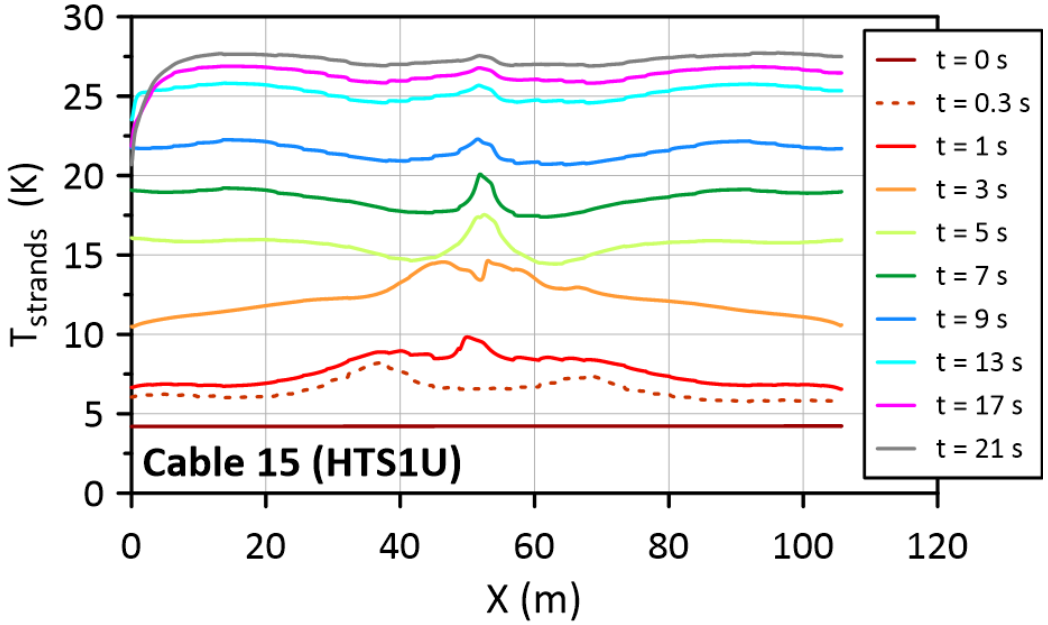

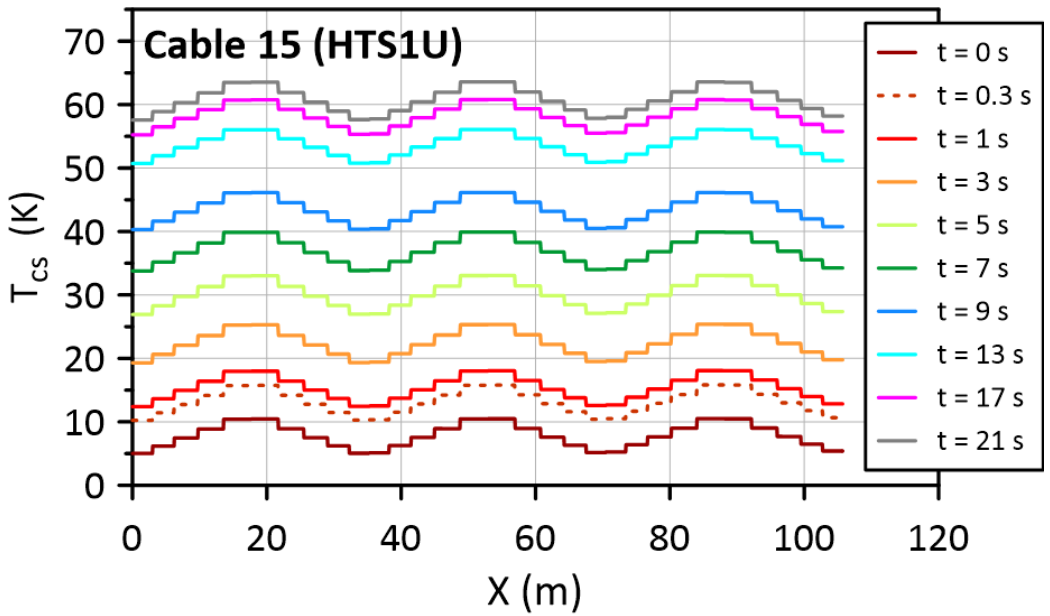

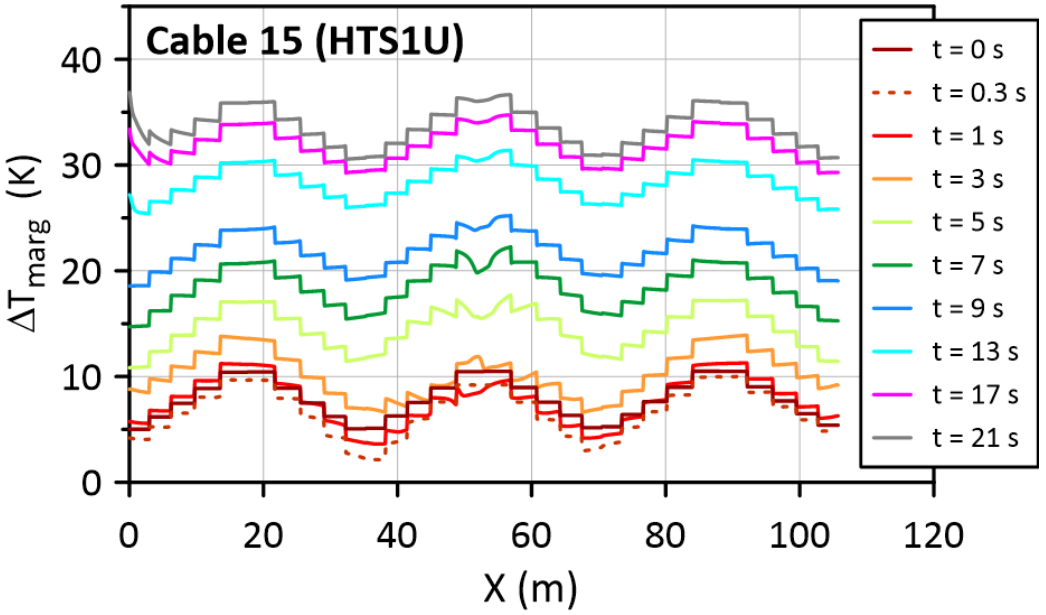

- In the first 20 s of the current scenario the conductor temperature and T_{cs} rise very fast, both affecting the ΔT_{marg} profile evolution.
- **The T_{max} value was of about 28 K.**
- At the very beginning (first 0.3 s) the temperature rise is faster, so the temperature margin slightly decreases, but later the T_{cs} rise becomes dominant.
- For each stored time step, we analysed the ΔT_{marg} profile along the considered conductor, seeking the minimum ΔT_{marg} value (in space).

Results - min ΔT_{marg} evolution during the whole current scenario

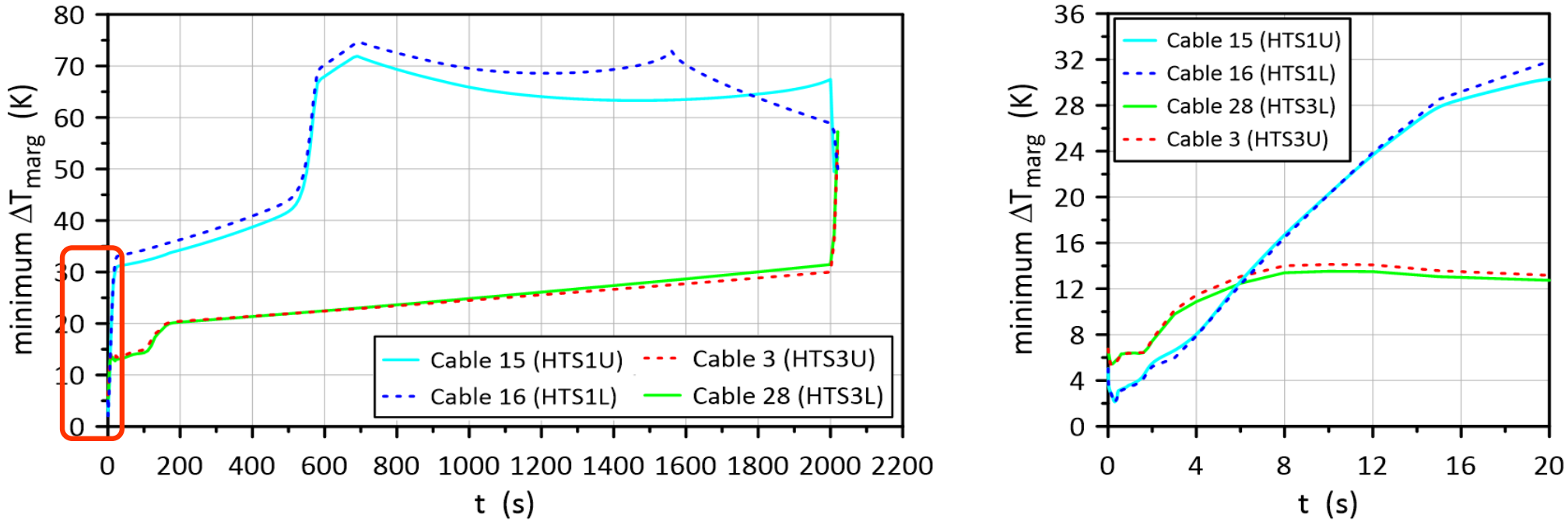

Time evolution of the min ΔT_{marg} for all considered conductors during the whole current scenario and its exargerated initial part.

- The global minimum (in time and space) of ΔT_{marg} was observed at t ≈ 0.22 s in the cables 3 and 28, and at t ≈ 0.30 in the cables 15 and 16.
- The lowest ΔT_{marg} value (2.068 K) was obtained for the Cable 16.
- In all considered conductors the global minimum ΔT_{marg} was sufficiently large (above 1.5 K), although we used a very conservative $I_c(B,T)$ scaling law. It was expected that the min ΔT_{marg} of the BEST conductors made of currently produced high performance HTS tapes would only be much higher.

Experimental T_{cs} values [9] vs. predictions of the adopted $I_c(B,T)$ scaling laws

$$I_{c1}(B,T) = n_t \cdot 2066.52 \cdot B^{-0.55666} \cdot \exp\left(\frac{-T}{39.2586 - 0.80338 \cdot B}\right)$$

$$I_{c2}(B,T) = \frac{F_{p0}}{B}\left[\frac{B}{B^*_{sc}(T)}\right]^p \left[1 - \frac{B}{B^*_{sc}(T)}\right]^q$$

$$F_{p0}(T) = A_0\left[1 - \left(\frac{T}{T_c}\right)^\beta\right] B^*_{sc}(T)^\nu$$

$$B^*_{sc}(T) = B_{sc0}\left[1 - \left(\frac{T}{T_c}\right)^\alpha\right]^\mu$$

A_0=21.24 $AT^{1-\nu}/cm$, B_{sc0} = 187.7 T, T_c=92 K, β=6.87,

α = 0.514, μ = 1.496, ν = 1.514, p = 0.521, q = 1.9

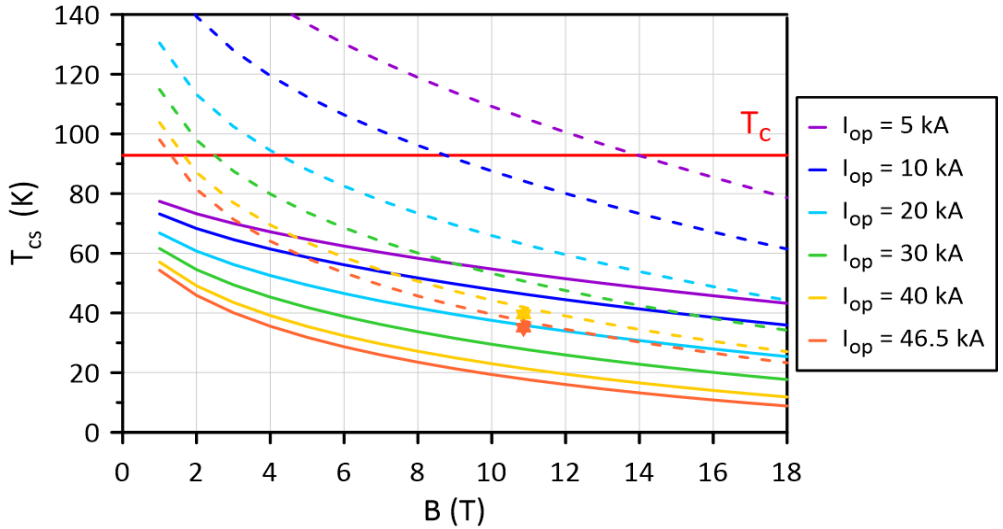

T_{cs} as a function of MF, resulting from the scaling laws I_{c1} (dashed lines) and I_{c2} (solid lines). The experimental values measured in SULTAN for the BEST conductor prototype are indicated by the star symbol.

The scaling law I_{c2} (B,T) is inapropriate for quench simulations (highly underestimated ΔT_{marg} => overestimated quench propagation velocity => underestimated quench detection time and the hot spot temperature)

We retained the general form of the 2nd scaling law but we adjusted the A_0 value to get the best agreement with the experimental T_{cs} values (**A_0=49.33 $AT^{1-\nu}/cm$**).

[9] X. Guanyu, *Progress on HTS magnet technology development*, presented at the Seminar on High-Temperature Superconducting Magnets within EU-CN Cooperation, Shanghai, 07.11.2025.

Quench simulations (ongoing)

- Cable 16 (HTS1L), in which the lowest global (in space and time) ΔT_{marg} minimum was reached, was selected to perform quench simulations.
- Quench is triggered by a heat pulse of length 0.1 m, duration 0.1 s and energy of twice Minimum Quench Energy (MQE) imposed at the location of the global min ΔT_{marg} at the very beginning of the current cycle.
- MQE is being estimated by trial and error procedure.
- After applying the heat disturbance, the operating current and magnetic field follows the normal scenario until the quench detection (i.e. exceeding the threshold voltage of **0.1 V**) plus additional delay t_{delay} = 1.1 s (corresponding to typical time necessary for reaction of the quench protection system), after which the exponential current dump starts with the characteristic time **τ = 0.814 s** [10]. The MF profile is also dumped proportionally to the operating current.
- Two cases are planned to be considered (with inter-turn and inter-pancake heat transfer taken into account or not)

[10] Y. Chen, et al., *Simulation of Quench Behavior in CS LTS Magnets for Next-Generation Fusion Devices With Time-Varying Operation*. IEEE Trans. Appl. Supercond. 35 (2025) Art. No. 4203209.

Summary, conclusion and perspectives

- THEA model of the BEST CS HTS conductor, and the dedicated UserMagneticField, UserCurrent and UserSHeating procedures for simulations of conductors' normal operation have been prepared and validated.
- We selected BEST CS conductors, which are subjected to the most demanding operating conditions, and we simulated their thermal-hydraulic behaviour at normal operation during the entire current scenario. Heat loads due to the magnetization, coupling and eddy current AC losses were taken into account.
- The global minima of the temperature margin for all considered conductors were observed in the first second of the current scenario. They were all above the 1.5 K performance criterion, even though the T_{cs} was estimated with a very conservative $I_c(B,T)$ scaling law.
- **Based on a comparison of the T_{cs} values predicted by both scaling laws with those measured for the conductor prototype, the lowest temperature margin within the entire HTS section of the actual CS coil is expected to fall within the range of 17–19 K, which is sufficiently large for its safe operation.**
- **However, the HTS conductors in the HTS1U/HTS1L modules reached peak temperatures of ~ 28 K. This significant thermal load poses a risk of heat diffusion to the adjacent LTS modules. Further, more comprehensive analysis of the integrated HTS/LTS system would be desirable.**
- The poster: M. Lewandowska, A. Dembkowska, R. Ortwein, G. De Marzi: Thermal-hydraulic analysis of the HTS part of the hybrid Central Solenoid designed for the next generation experimental fusion device, was presented at ISFNT 2025, and the respective paper was submitted to Fusion Eng. Des.
- Quench simulations in the Cable 16 (HTS1L) are ongoing.

Thank you very much for your attention

This work has been carried out within the framework of the EUROfusion Consortium, funded by the European Union via the Euratom Research and Training Programme (Grant Agreement No 101052200 — EUROfusion). Views and opinions expressed are however those of the author(s) only and do not necessarily reflect those of the European Union or the European Commission. Neither the European Union nor the European Commission can be held responsible for them.
This work has been co-financed by the Polish Ministry of Science and Higher Education in the framework of the International Co-financed Projects (PMW) programme in the year 2025 (contract number 6265/HE - EURATOM/2025/2).